

Turbulence-aberration correction with high-speed high-gain optical phase conjugation in sodium vapor

V. S. Sudarshanam and M. Cronin-Golomb

Electro-Optics Technology Center, Tufts University, 4 Colby Street, Medford, Massachusetts 02155

P. R. Hemmer

Rome Laboratory, Hanscom Air Force Base, Bedford, Massachusetts 01731

M. S. Shahriar

Research Laboratory of Electronics, Massachusetts Institute of Technology, Cambridge, Massachusetts 02139

Received March 31, 1997

Optical aberrations that are due to high-speed turbulence in the aero-optical regime are corrected with optical phase conjugation based on coherent population trapping in sodium vapor. Experimental measurements of an unheated, forced helium jet in air have demonstrated aberration correction by a factor of 7.8 at a forcing frequency of 18 kHz with an optical power gain of 32. © 1997 Optical Society of America

Adaptive-optic systems can correct for turbulence aberrations in the atmospheric propagation regime at speeds as fast as 300 Hz. However, in the aero-optical regime of turbulence, the required bandwidth¹ is as much as 100 kHz. It was suggested² that optical phase conjugation should be capable of correcting aberrations that are due to turbulence. However, most existing nonlinear-optical materials, for example, photorefractive media,³ have a sufficiently fast response only if high-peak-power pump beams are used, which requires pulsed lasers. Real-time compensation of atmospheric turbulence by four-wave mixing (FWM) in sodium (Na) vapor with cw lasers of 20 W/cm² was demonstrated.⁴ However, the conjugate gain was only 0.2. In this Letter we demonstrate the use of cw lasers with low intensities of the order of 5 W/cm² to perform high-speed spatiotemporal aberration correction and still achieve a high phase-conjugate gain of 32.

Previously we reported⁵ a high conjugate gain with a response faster than 1 μ s when Gaussian beams and low pump intensities of ~ 1 W/cm² were used. These results were achieved in an externally pumped FWM configuration by use of the mechanism of coherent population trapping⁵⁻⁹ (CPT) in Na vapor. Such low pump intensities could be used because the optical nonlinearity saturates at an intensity below that needed to saturate the optical transition. Here we show that this performance does not degrade in the presence of large-angle aberrations caused by a turbulent jet flow.

The FWM configuration for aberration correction in Na vapor is shown schematically in Fig. 1. Two different ring dye lasers (linewidths ~ 3 MHz) tuned approximately to the D_1 transition are used to produce the forward, F, and the backward, B, pumps. Probe beam P is derived from F by use of an acousto-optic modulator (AOM) configured for upshifting the frequency by 1.772 GHz, which is equal to the ground-state hyperfine transition frequency of Na. This method of using an acousto-optic modulator ensures that the laser jitters of F and P are correlated as required

for efficient CPT.¹⁰ In this FWM configuration⁵ the conjugate beam, C, is produced when B scatters off the grating formed by F and P. Probe beam P makes an angle of ~ 5 mrad with pump F in the vertical plane. To avoid laser feedback, we misaligned counter-propagating pump beams F and B by ~ 1 mrad in the horizontal plane. The typical optical intensity of the collimated F and B beams is ~ 4.9 W/cm² and that of the weaker P beam is ~ 1.3 mW/cm². Typical FWHM spot sizes of the F, B, and P beams are roughly 1.2, 1.3, and 0.7 mm, respectively, at the center of the Na cell. The F and B pumps have an identical linear polarization, but P is cross polarized and steered into the cell by a polarizing beam splitter (PBS), as shown in Fig. 1. The Na-vapor cell is a heat-pipe oven operated at ~ 215 °C with an ambient background pressure of ~ 13 mTorr. No buffer gas is added to the cell. Magnetic shielding is used to reduce stray magnetic fields to smaller than 100 mG.

As shown in the inset of Fig. 1, probe beam P is passed through an unheated turbulent helium gas jet in air. We arrange lens L, with a focal length of 17.5 cm, in an approximate 4*f* configuration to image this jet into the active region of the cell with a

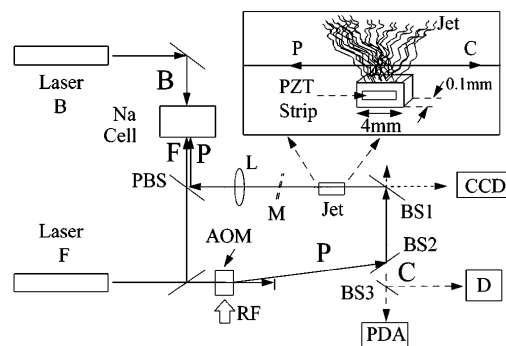


Fig. 1. Schematic diagram of the experimental setup for turbulence-aberration correction with a FWM-based Na-vapor phase-conjugate mirror.

slight demagnification. This imaging action ensures that the aberrated probe beam size at the cell center (<0.8 mm) is smaller than the size of pump beams. We produce the turbulent jet by forcing helium gas at room temperature through a rectangular nozzle ($4 \text{ mm} \times 0.125 \text{ mm}$) aligned with the 4-mm side of the nozzle along the path of P (see the inset in Fig. 1). The nozzle is located ~ 2 mm below the probe beam path, at a distance of ~ 70 cm from the center of the Na cell. The average helium flow velocity at the nozzle exit is estimated from the volume flow rate of 11 cubic feet per hour and the area of the nozzle (0.5 mm^2) to be ~ 170 m/s.

As shown in Fig. 1 conjugate beam C is picked off first at beam splitter BS1 to be viewed through a CCD camera and second at BS2 to be detected simultaneously at photodetector D for power-gain measurements and at a pinhole-detector assembly (PDA) for temporal aberration effects. The PDA is ~ 164 cm from the nozzle center and consists of a pinhole (0.2-mm diameter) placed 1 mm in front of a photodetector. Turbulence aberration is measured when probe beam P makes a single pass through the helium jet and is reflected onto the PDA and the CCD by a removable mirror, M. Mirror M is adjusted ~ 0.1 rad from the perpendicular to P to ensure that the P beam does not make a second pass through the jet.

To facilitate quantitative measurements of the temporal aberrations induced by the turbulent jet, we vibrate the nozzle by use of a piezoelectric lead zirconium titanate transducer (PZT). It is known¹¹ that eddy structures in turbulent jets are sensitive to harmonic forcing, thus providing an easy way of studying them.¹² It is also known¹³ from hot-wire oscillograms for a helium jet that turbulence aberrations arise from the density difference between helium and air. Thus the light intensity seen at the PDA is modulated by the turbulent jet at the PZT forcing frequency. The transverse position of the pinhole of the PDA is adjusted for maximum ac amplitude on the photodetector signal of the PDA at the forcing frequency. The ratio of this peak-to-peak ac voltage to the maximum voltage level is termed the modulation depth. This modulation depth is chosen as the experimental measure of the temporal aberration at the forcing frequency because it compensates for the difference in the intensities of the conjugate and the probe beams.

A strong resonance in the modulation depth was measured at a forcing frequency of 17.8 kHz. Forcing frequencies as high as 75 kHz were tried. Appreciable ac amplitude in the PDA output was obtained at forcing frequencies of 43, 54, and 68 kHz, but in these cases the PDA signal showed temporal aberrations only at a subharmonic of the forcing frequency. The mechanism of subharmonic generation can be probably related to eddy behavior reported by others.¹² As a result of the subharmonic generation, we chose to make our measurements at the 17.8-kHz resonance because it provided a clean, large-amplitude PDA signal.

The plots of the instantaneous output voltage from the PDA are displayed in Fig. 2 for the probe and the conjugate beams. Trace (a) of Fig. 2 shows the electrical input signal at 17.8 kHz applied to the PZT

strip on the jet nozzle. Trace (b) shows the optical effect of turbulence on probe P after a single pass through the helium jet. Trace (c) shows the optical effect of the turbulence on conjugate C that has very closely retraced the path of P, traveling back through the turbulent flow. From these data, the signal-modulation depth, as defined above, is estimated at 63% for P but at only 8% for C. This demonstrates that turbulence aberrations in the conjugate beam are corrected by a factor of 7.8.

Time-averaged spatial aberration correction is demonstrated in Fig. 3 through images captured with the CCD camera. The profile of conjugate C after a single pass through the turbulent helium jet is shown in the two-dimensional contour plot and the one-dimensional line trace in Fig. 3(a). As can be seen, a well-corrected nearly circular spot is observed. Here the conjugate gain is ~ 32 . This profile of the conjugate beam under flow is to be compared with the profile of probe P in Fig. 3(b) after a single pass

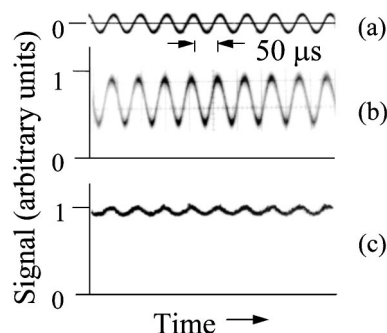


Fig. 2. Temporal-aberration correction: (a) electrical input signal at 17.82 kHz applied to a PZT strip, (b) aberrated probe signal at the PDA after a single pass through the helium jet, and (c) corrected conjugate signal at the PDA after retraversal through the jet.

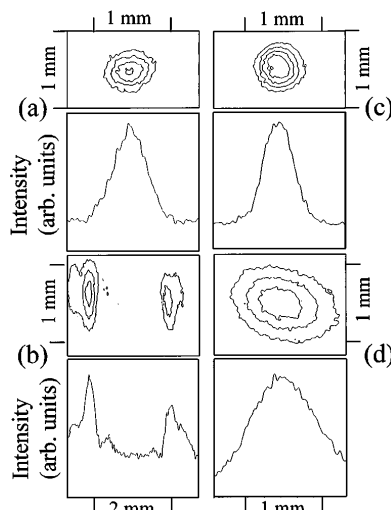


Fig. 3. Spatial-aberration correction: two-dimensional contours (upper plots) and one-dimensional line traces (lower plots) of the spatial intensity distribution of (a) the conjugate beam with helium flow ON, (b) the probe beam with helium flow ON, (c) the conjugate beam with helium flow OFF, and (d) the probe beam with helium flow OFF. Contours in (a) and (c) are drawn at 80%, 60%, 40%, and 20% of the peak intensity, whereas in (b) and (d) they are drawn at 75%, 50%, and 25% of the peak intensity.

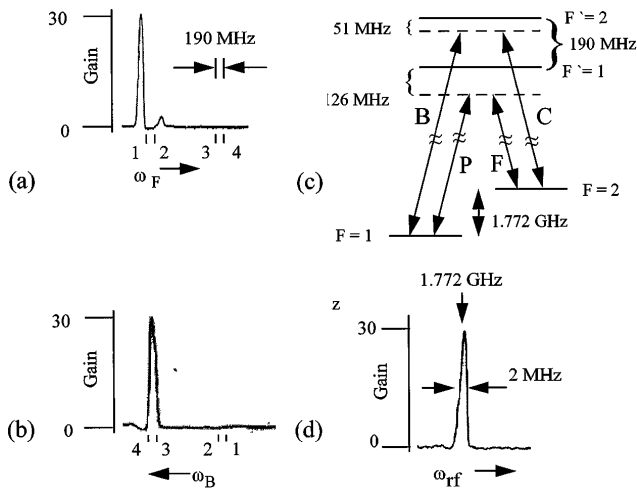


Fig. 4. Conjugate gain as a function of (a) frequency ω_F , (b) frequency ω_B , and (d) frequency ω_{rf} . The energy-level diagram for the transitions that are proposed is shown in (c). The numbers 1–4 in (a) and (b) correspond to the following transitions: (1) $F = 2 \leftrightarrow F' = 1$ (2) $F = 2 \leftrightarrow F' = 2$, (3) $F = 1 \leftrightarrow F' = 1$, and (4) $F = 1 \leftrightarrow F' = 2$.

through the turbulent jet. Note the large aberration and the distinct far-field flow pattern. The extent and the geometry of the flow pattern are dependent on drive frequency, flow velocity, distance of the nozzle exit plane from the probe beam, and jet alignment with respect to the probe beam. For comparison, Fig. 3(c) shows the profile of conjugate C when the helium flow is cut off. Here the gain is ~ 45 . This shows that the aberration did not excessively degrade the conjugate performance. Finally, Fig. 3(d) shows the profile of probe P without flow. The size of P as shown in Fig. 3 is larger than that of C because P was divergent as it approached the jet and was recorded 77 cm downstream from the nozzle, whereas C was recorded 65 cm upstream from the nozzle.

Fig. 4(a) shows the conjugate gain as a function of the frequency ω_F (laser F) in the presence of helium flow, with the frequency ω_B (laser B) tuned for maximum gain. Figure 4(b) shows the phase-conjugate gain as a function of the frequency ω_B , with ω_F kept tuned for maximum gain. The FWHM of the gain peaks in Figs. 4(a) and 4(b) was measured to be 118 and 127 MHz, respectively. The maximum conjugate gain occurred when F and B (P and C) were tuned as shown in Fig. 4(c). A slightly smaller conjugate gain of ~ 26 was obtained when F was blue detuned 126 MHz from the $F = 2$ to the $F' = 2$ transition and B was red detuned 190 MHz from the $F = 1$ to the $F' = 1$ transition. It should be noted that the Doppler width of Na vapor at 215 °C is ~ 1 GHz, so the frequencies noted in Fig. 4 apply to only the zero-velocity group in the vapor.

To confirm that the gain mechanism in these measurements is indeed CPT, we determined the two-photon resonance width by scanning the frequency ω_{RF} of the AOM (see Fig. 1) and measuring the linewidth of the gain. This is shown in Fig. 4(d), again in the presence of the helium flow. As can be seen, the FWHM of the gain is 2 MHz, which is smaller than the

10-MHz natural linewidth of Na. This subnatural radio-frequency linewidth provides evidence of CPT.^{5,9}

An estimate of the phase-conjugate response time can be obtained from the reciprocal of the linewidth, which as shown in Fig. 4(d) was found to be 79 ns. This is much faster than the forcing frequency of 17.8 kHz set by the particular characteristics of the PZT–nozzle assembly, and hence the temporal aberration-correction factor of 7.8 as shown in Fig. 2 is probably not limited by the phase-conjugate response time. To explain lack of complete correction, we note that earlier reports² showed that pump misalignments can greatly reduce the amount of aberration correction otherwise possible in an ideally counterpropagating configuration. As already mentioned, we slightly misaligned the F and the B beams in our experimental setup to avoid instabilities arising from laser feedback. However, this feedback problem can be overcome by use of optical isolators.

In conclusion, high-speed aero-optical turbulence aberrations at a frequency of 18 kHz have been corrected for by a factor of 7.8 with a high gain 32 by use of low-power cw lasers. This was accomplished with CPT-based phase conjugation in Na vapor in a FWM configuration.

The authors thank S. Ezekiel of the Massachusetts Institute of Technology. This research was sponsored by the U.S. Air Force Rome Laboratory through grants F30602-96-2-0101 and F30602-96-2-0100.

References

1. R. J. Hugo and E. J. Jumper, *Appl. Opt.* **35**, 4436 (1996).
2. See, for example, R. A. Fisher, ed., *Optical Phase Conjugation* (Academic, New York, 1983), Chap. 14.
3. See, for example, B. Monson, G. J. Salamo, A. G. Mott, M. J. Miller, E. J. Sharp, W. W. Clark III, G. L. Wood, and R. R. Neurgaonkar, *Opt. Lett.* **15**, 12 (1990).
4. R. C. Lind and G. J. Dunning, *Laser Focus/Electro-Optics* **9**(19), 14 (1983).
5. P. R. Hemmer, D. P. Katz, J. Donoghue, M. Cronin-Golomb, M. S. Shahriar, and P. Kumar, *Opt. Lett.* **20**, 982 (1995).
6. G. Alzetta, A. Gozzini, L. Moi, and G. Orriols, *Nuovo Cimento B* **36**, 5 (1976).
7. H. R. Gray, R. M. Whitley, and C. R. Stroud, *Opt. Lett.* **3**, 218 (1978).
8. P. M. Radmore and P. L. Knight, *J. Phys. B* **15**, 3405 (1982).
9. J. Donoghue, M. Cronin-Golomb, J. S. Kane, and P. R. Hemmer, *Opt. Lett.* **16**, 1313 (1991).
10. J. E. Thomas, P. R. Hemmer, S. Ezekiel, C. C. Leiby, Jr., R. H. Picard, and C. R. Willis, *Phys. Rev. Lett.* **48**, 867 (1982).
11. S. C. Crow and F. H. Champagne, *J. Fluid Mech.* **48**, 547 (1971).
12. A. K. M. F. Hussain and K. M. B. Q. Zaman, in *Proceedings of the Symposium on Turbulence*, H. Fiedler, ed., Vol. 75 of *Lecture Notes in Physics* (Springer-Verlag, Berlin, 1978), p. 31.
13. R. Riva, G. Binder, S. Tardu, and M. Favre-Marinet, in *Turbulence and Coherent Structures*, O. Metais and M. Lesieur, eds. (Kluwer Academic, Dordrecht, The Netherlands, 1991).